Bending characteristics of dual-hole PM-PCF based on LP_{01} and LP_{11} modal interference*

GUO Xuan (郭璇)**, **LIU Feng** (刘丰), **GAO Meng-yuan** (高梦圆), **TAN Ai-ling** (谈爱玲), **FU Xing-hu** (付兴虎), **and BI Wei-hong** (毕卫红)

The Key Laboratory for Special Fiber and Fiber Sensor of Hebei Province, School of Information Science and Engineering, Yanshan University, Qinhuangdao 066004, China

(Received 6 January 2016)

The bending characteristics of dual-hole polarization maintaining photonic crystal fiber (PM-PCF) are demonstrated in this paper. The modal interference is induced by the LP_{01} mode and LP_{11} mode propagating in a single PM-PCF with the same polarization direction. Simulation results demonstrate that the bending radius induces the phase difference between LP_{01} mode and LP_{11} mode, which leads to the change of light interference intensity on the fiber output facet. The relationship between bending radius and normalized interference intensity with three different bending angles is discussed, where the bending angle is defined as the angle between hole axis and the *x* axis. The bending sensitivity is obtained to be about −188.78/m around the bending radius of 1.5 cm with the bending angle of 90°. The bending characteristics can contribute for online bending detection in widespread areas.

Document code: A **Article ID:** 1673-1905(2016)02-0136-4

DOI 10.1007/s11801-016-6002-9

As a novel device, optical fiber curvature sensor plays an important role in several areas, such as structure health monitoring, aerospace and geophysics[1-4]. Due to the particular advantages of immunity to electromagnetic interference, corrosion resistance, compact structure and high sensitivity, the optical fiber curvature sensor can be used in some adverse conditions[5-7]. Over the past few years, various optical fiber sensors used for curvature measurement have been reported, such as fiber gratings[8,9], Sagnac loop based on polarization maintaining fiber (PMF)[10], two-core fiber interferometer[11] and other structures. But the sensors mentioned above are hindered by the complicated demodulation system and complex manufacture. Thus, it is significant to develop a simple bending sensor structure with easy demodulation method and low cost.

At present, the PMFs based on the mode interference between *x* component and *y* component of LP_{01} mode are widely provided in strain, voltage and liquid refractive index measurement[12-14]. However, there are few reports about the curvature characteristics of PMF, especially for the polarization maintaining photonic crystal fiber (PM-PCF), based on the modal interference of LP_{01} mode and LP_{11} mode in the same direction (*x* or *y* orientation), which can be easily detected by output light intensity. In this paper, the PCF with two big holes is proposed for bending sensing. Depending on the interference intensity distribution of PM-PCF, which is modulated by the bending curvature, the output intensities of two lobes will exchange as the bending radius changes. Moreover, the light intensity detection is simpler than the wavelength demodulation, which overcomes the obstacle of complicated and expensive demodulation system. The bending characteristics are thoroughly discussed in this paper. The results show that the sensing section of the PMF is about 3 cm in length, and the bending sensitivity of measurement is about −188.78/m around the bending radius of 1.5 cm with the bending angle of 90°.

Based on intermodal interference theory, if the linear polarization modes of LP_{01} mode and LP_{11} mode simultaneously exist in the fiber, they will interfere with each other, and the output light intensity is decided by[15]:

$$I = \left|E(x,y)\right|^2 = E_{01}^2 + E_{11}^2 + 2E_{01}E_{11}\cos(\Delta\phi), \quad (1)$$

where E_{01} and E_{11} are the electric field intensities of LP_{01} and LP_{11} modes, respectively, and $\Delta\varphi$ is the phase difference of the two modes. The fiber analyzed in this paper is PM-1550-01 PM-PCF which was purchased from Crystal Fiber A/S Inc. The microscope image and schematic diagram of the fiber are shown in Fig.1(a) and (b), respectively.

* This work has been supported by the National Natural Science Foundation of China (No.61475133), the Hebei Provincial Natural Science Foundation (No.F2015203270), the Yanshan University Doctor Foundation (No.B872), the Yanshan University Youth Foundation (No.14LGB015), the College Youth Talent Project of Hebei Province (No.BJ2014057), and the Hebei Educational Committee Natural Science Youth Fund (No.QN2014034).

** E-mail: guoxuan@ysu.edu.cn

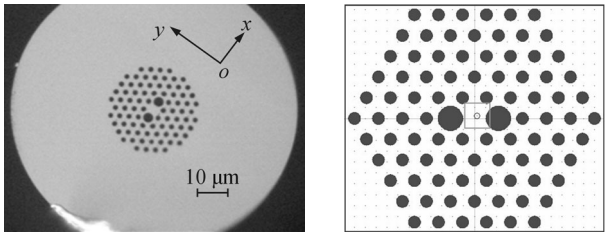

Fig.1 (a) Microscope image and (b) schematic diagram of PM-PCF

The outer holes diameter is 2.2 μm, and the inner big holes diameter is 4.5 μm. The hole to hole pitch Λ is 4.4 μm. The background material is pure silica, and the Sellmeier equation is used for calculating the chromatic dispersion of silica. The cladding holes are filled with air (n_{air}=1.0). Because of the two big holes, the symmetrical structure is disturbed. As a result, the modes in the fiber exhibit polarization maintaining characteristic. For example, there are four polarization modes at 640 nm, namely, LP_{01}^{x}, LP_{01}^{y}, LP_{11}^{x} and LP_{11}^{y}. The electric field distributions of LP_{01}^{y} and LP_{11}^{y} modes are shown in Fig.2.

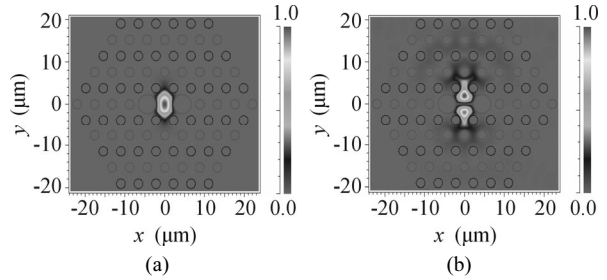

Fig.2 Electric field distributions of (a) LP_{01}^{y} mode and (b) LP_{11}^{y} mode

The intermodal phase difference $\Delta\varphi$ is defined by:

$$\Delta\phi = \Delta\beta \cdot L = \frac{2\pi}{\lambda}\left(n_{\text{eff}}^{01} - n_{\text{eff}}^{11}\right), \tag{2}$$

where n_{eff}^{01} and n_{eff}^{11} are the effective indices of the two modes. Eq.(2) indicates that the output light intensity varies sharply with $\Delta\varphi$. Fig.3 illustrates the intensity patterns for $\Delta\varphi$ changing from 0° to 360°.

When the sensor length L remains unchanged, the parameter $\Delta\varphi$ is only decided by the effective refractive index. When the bending radius of the fiber changes, n_{eff}^{01} and n_{eff}^{11} will change accordingly. In this case, if the intensity of one or two lobes is monitored, the phase difference can be obtained and the phase difference shift caused by bending can be measured.

The relationship between the bending radius and the output intensity pattern with three bending angles (0°, 60° and 90°) will be simulated. The bending angle is the angle between the two big holes axis and the x axis. The y orientation is the bending direction, as shown in Fig.4.

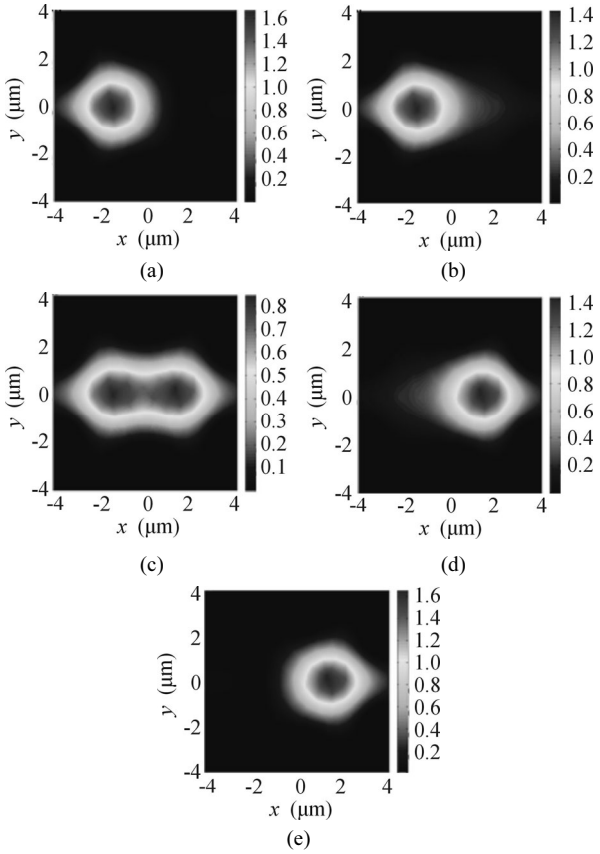

Fig.3 The output light intensities with different $\Delta\varphi$: (a) 0°; (b) 60°; (c) 90°; (d) 120°; (e) 180°

A 640 nm light source is chosen for analysis. When the fiber sensor is disturbed by bending, the output intensity pattern is changed as shown in Fig.5 with the bending angle of 60°. From Fig.5, it can be seen that the two-lobe energy exchanges as the bending radius changes. When the bending radius increases from 1 cm to 1.75 cm, the right lobe intensity is weakened gradually, while the left lobe intensity increases obviously.

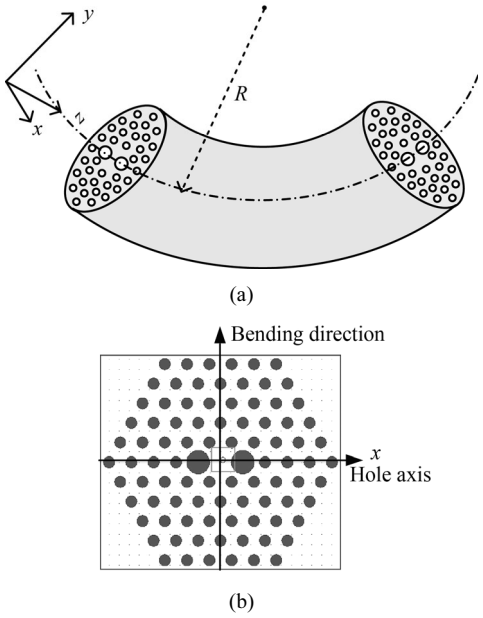

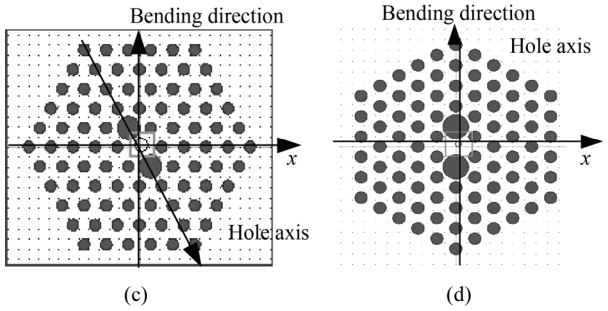

Fig.4 (a) The bending schematic and output intensity patterns with different bending angles of (b) 0°, (c) 60° and (d) 90°

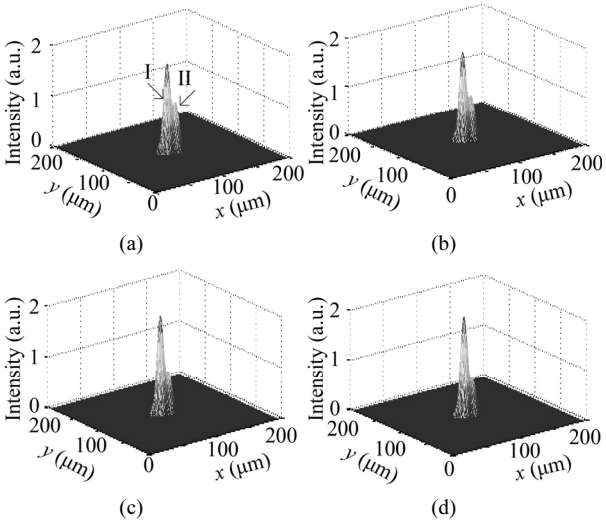

Fig.5 The output intensities with different bending radii of (a) 1 cm, (b) 1.25 cm, (c) 1.5 cm and (d) 1.75 cm (I-Left, II-Right)

The normalized intensity is defined as the difference to the sum of the two-lobe intensities, which is expressed as:

$$N = \frac{I_{\text{Left}} - I_{\text{Right}}}{I_{\text{Left}} + I_{\text{Right}}}, \tag{3}$$

where I_{Left} is the intensity of the left lobe which is obtained by integral method, and I_{Right} is the right one. The value indicates the output energy exchange of the two lobes. The relationship between the normalized intensity and bending radius is analyzed with the bending angles of 0°, 60° and 90°, which is shown in Fig.6.

From Fig.6, it can be seen that the relation curves show parabola with three bending angles. When the angle between hole axis and x axis is equal to 0°, the normalized intensity increases as the bending radius varies from 1.00 cm to 1.27 cm. However, it decreases monotonously with the bending radius ranging from 1.27 cm to 2 cm. There are the similar variation trends when bending angles are 60° and 90°. Moreover, it realizes the high sensitivity of −188.78/m around 1.5 cm bending radius when the bending angle is 90°, which is much higher than −46.89/m at 0°. Furthermore, it is noted that the normalized intensity is decided by the length and the initial state of the sensor. The curve slope which represents the sensitivity is more important for sensor selection.

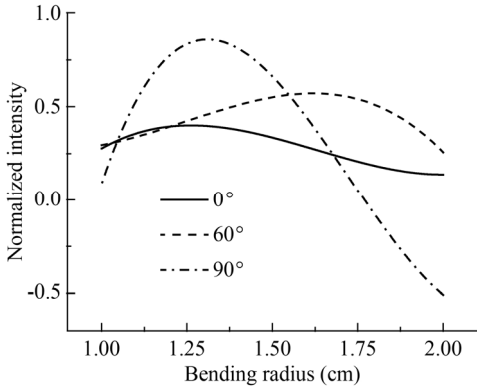

Fig.6 The relationship between the normalized intensity and bending radius with different bending angles

A detection system is set up for testing. Fig.7 shows the output interference spots of the two-hole PCF with the 640 nm light source. When the fiber is subjected to bending, the right spot's intensity increases, while the left one decreases in contrast.

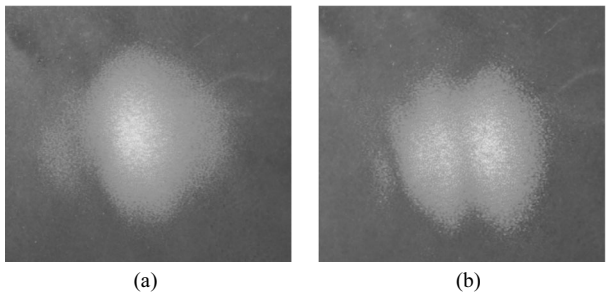

Fig.7 The output interference spots of the PM-PCF (a) before and (b) after bending

The normalized intensity is transformed to voltage value in the experiment by processing unit. When the wavelength is fixed at 640 nm, the relationship between the output voltage and bending radius with the bending angle of 90° is shown in Fig.8.

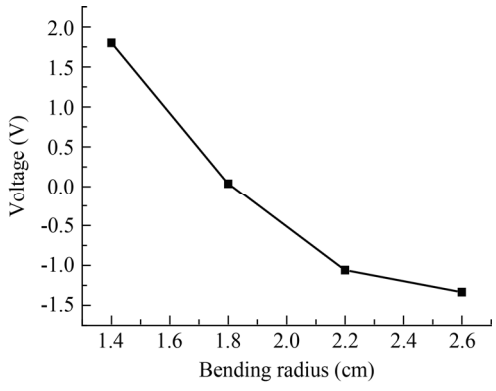

Fig.8 The relationship between the output voltage and the bending radius

The results show that when the radius increases from 1.4 cm to 2.6 cm, the voltage keeps the same trend as Fig.6. Therefore, simulation results are verified by the experiment. Besides, the detection sensitivity can be improved by choosing sensitive photo-detection and high-factor amplified circuit.

The bending characteristics of the two-hole PM-PCF are analyzed in this paper. The interference between LP_{01} mode and LP_{11} mode is investigated based on the beam propagation method. And then the bending characteristics are experimentally demonstrated. The simulation results indicate that the sensor with length of 3 cm has the sensitivity about −188.78/m around bending radius of 1.5 cm with the bending angle of 90°. The sensor has the features of high sensitivity, high stability, compact structure and simple detection system. It is expected to be applied in bending sensing in different solutions.

References

[1] J. R. Guzman-Sepulveda, M. Torres-Cisneros, R. Guzman-Cabrera and D. A. May-Arrioja, Highly Sensitive Fiber Optic Curvature Sensor, Frontiers in Optics, FTh2B.3 (2013).

[2] LI Hong-cai, LIU Chun-tong, FENG Yong-bao, ZHOU Zhao-fa and HE Zhen-xin, Journal of Optoelectronics·Laser **26**, 309 (2015). (in Chinese)

[3] Zhilong Ou, Yongqin Yu, Peiguang Yan, Jishun Wang, Quandong Huang, Xue Chen, Chenlin Du and Huifeng Wei, Optics Express **21**, 23812 (2013).

[4] Mohd Anwar Zawawi, Sinead O'Keeffe and Elfed Lewis, Journal of Lightwave Technology **33**, 2492 (2015).

[5] H. Qu, G. F. Yan and M. Skorobogatiy, Optics Letters **39**, 4835 (2014).

[6] G. Salceda-Delgado, A. Van Newkirk, J. E. Antonio-Lopez, A. Martinez-Rios, A. Schülzgen and R. Amezcua Correa, Optics Letters **40**, 1468 (2015).

[7] Cao Ye, Liu Hui-ying, Tong Zheng-rong, Yuan Shuo and Zhao Shun, Optoelectronics Letters **11**, 0069 (2015).

[8] Pouneh Saffari, Thomas Allsop, Adedotum Adebayo, David Webb, Roger Haynes and Martin M. Roth, Optics Letters **39**, 3508 (2014).

[9] Shijie Zheng, Baohua Shan, Masoud Ghandehari and Jinping Ou, Measurment **72**, 43 (2015).

[10] Yu Zhao, Yongxing Jin, Huaping Gong and Jianfeng Wang, The Curvature Measurement of Sagnac Loop based on PMF, Asia Communications and Photonics Conference and Exhibition, 79900S-1 (2010).

[11] J. R. Guzmán-Sepúlveda, M. A. Fuentes-Fuentes, J. J. Sanchez-Mondragon and D. A. May Arrioja, High-sensitivity Curvature Sensor based on Two-Core Fiber, Latin America Optics and Photonics Conference, LTh2C.5 (2012).

[12] Jiang Ying, Zeng Jie, Liang Dakai, Ni Xiaoyu and Zhou Yabin, Acta Optica Sinica **33**, 1106001 (2013). (in Chinese)

[13] X Y Dong, H Y Tam and P Shum, Appl. Phys. Lett. **90**, 151113 (2007).

[14] Wu Tiesheng, Wang Li, Wang Zhe, Liu Yumin, Hu Shuyang and Yin Lidan, Chinese Journal of Lasers **39**, 1114002 (2012). (in Chinese)

[15] Feng Liu, Delan Cao, Xuan Guo and Xin Lu, Chinese Optics Letters **10**, 050603 (2012).